THE IMPACT OF BEAM EMITTANCE ON BSM-PHYSICS DISCOVERY POTENTIAL AT A MUON COLLIDER

D. Greenwald*, A. Caldwell, Max Planck Institute for Physics, Munich, Germany

Abstract

A muon collider would allow for high precision probing of the multi-TeV energy regime and the potential discovery of new physics. Background radiation from electrons from the decay of muons interacting with the beam pipes near the interaction point (IP) places limitations on the design of a muon-collider detector. In particular, conical shielding extending out from the IP along the outside of the beam pipes prevents detection of particles at small angles to the beam line. For a given luminosity, bunches with smaller emittances will have fewer muons and therefore smaller background levels, allowing for shielding with shallower angles. The angular-acceptance dependence of the discovery potential for Kaluza-Klein excitations of the standard model particles is presented as a motivation for improved beam-cooling techniques that can achieve high luminosities with small bunch populations.

INTRODUCTION

A major challenge in the designing of a multi-TeV muon collider [1, 2] is the reduction of background signals in the interaction-point (IP) detectors. The largest source of background in the interaction region comes from electrons emitted by muons decaying upstream of the IP in the final focus region of the collider ring [1, 3]. These electrons follow the muon beam trajectory until they encounter a focusing magnetic, which deflects them out of the beam pipe. The high-energy electrons (10^2–10^3 GeV) radiate photons in the magnetic fields and produce showers of electrons, photons, hadrons, and muons, when they hit materials surrounding the beam pipe

It is important to shield the detector from these showers by ensuring that no active components of the detector are exposed to surfaces irradiated by decay electrons. The detectors must also be shielded against the neutrons and muons produced in the shielding itself.

A plan common to most muon collider studies places tungsten shielding inside and around the beam pipe in the detector region. The outside of the beam pipe is surrounded by a cone of tungsten that begins centimeters from the IP and radiates out along the beam line (figure 1). The angle at which the shielding could extend from the IP ranges between 9° and 30° in background studies.

While such shielding is necessary to run the detector, it may greatly impact the ability to precisely measure physical parameters. Alternatively, decreasing the muon beam emittance allows one to decrease the bunch population while keeping the luminosity constant. Decreased bunch population reduces the background rate, allowing for shallower shielding angles.

In this paper, we present a model of physics beyond the standard model (BSM) containing a single extra dimension accessible to all fields of the standard model (SM), and discuss the impact of limited angular acceptance in a detector on the detection of the model and the measurement of its defining parameter at a $\mu^+\mu^-$ collider.

* deg@mpp.mpg.de

UNIVERSAL EXTRA DIMENSIONS

The impacts of extra spatial dimensions on 4D physics were investigated early on by Kaluza [4] and Klein [5], with such theories now called Kaluza-Klein (KK) theories. Modern versions of these theories are characterized by the number and shape of extra dimensions and by which of the SM fields permeate them (see [6] or [7] for a good survey). In the theory of universal extra dimensions (UED), all SM fields propagate in additional flat compact dimensions [8]. The discrete excitations of SM fields in the extra dimensions appear as towers of heavier-mass states of the SM particles, with tree-level masses

$$m_n^2 = n^2 R^{-2} + m_{\mathrm{SM}}^2, \qquad n \in \mathbb{N},$$

where m_{SM} is the standard model mass, n the excitation level, and $R^{-1}$the inverse size of the extra dimensions, typically measured in GeV. The particle spectrum at each KK level n is highly mass degenerate at tree level, but is much richer, when loop-level contributions to the KK masses are included [9]: color-charged particles receive radiative mass contributions up to nearly 25% of R^{-1}, with the gluon being the heaviest KK_n particle; the KK hypercharge boson B_n (nearly identical to γ_n, for nonzero n) receives the smallest mass corrections and is the lightest KK_n particle.

We have investigated the simplest UED scenario that preserves the SM at the $n = 0$ level, which contains a single extra dimension compactified on a circle with $\mathbb{S}^1/\mathbb{Z}_2$ orbifolding to preserve SM chirality. This model contains a new parity charge, $P_{\mathrm{KK}} = (-1)^n$. Conservation of this

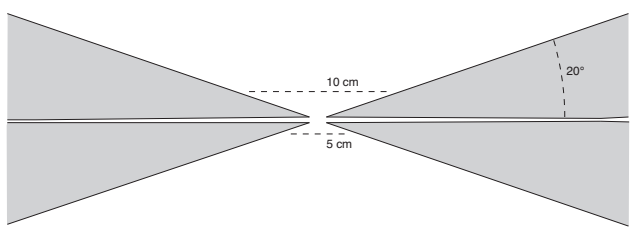

Figure 1: Tungsten shielding (to scale) around the interaction point (1.1 m shown on either side) with a 20° angle.

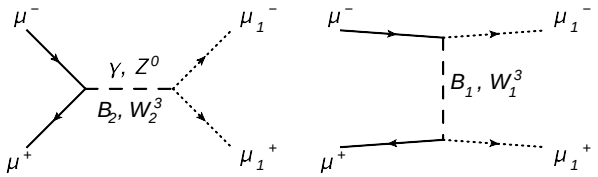

Figure 2: KK_1 muon pair production diagrams. The μ_1's decay to μ's and (undetected) B_1's.

parity (and KK number) requires that SM particles produce odd-n excitations in pairs only. Furthermore, KK number conservation suppresses the single production of even-n states. This results in lighter constraints on the size of an extra dimension than arise in other scenarios [6, 8]. Conservation of P_{KK} also means that the lightest KK_1 particle is stable, and therefore a dark matter candidate.

The range of R^{-1} of interest for this paper is several hundred GeV to 1.5 TeV. The other important parameters of the minimal UED (mUED) model are the cutoff scale Λ for the effective theory and the SM higgs mass. In the following calculations $\Lambda R = 20$ and we neglect higgs interactions.

UED AT A 3-TeV $\mu^+\mu^-$ COLLIDER

A clear signal of UED that can be observed at a muon collider is the production of a $\mu_1^+\mu_1^-$ pair (figure 2)

$$\mu^+\,\mu^- \;\rightarrow\; \mu_1^+\,\mu_1^- \;\rightarrow\; \mu^+\,\mu^-\,\mathrm{B}_1\,\mathrm{B}_1.$$

The counterpart process has been studied for an $\mathrm{e}^+\mathrm{e}^-$ collider (see for example [10]). The KK_1 muons decay promptly to SM muons and B_1 bosons. The B_1's exit the experiment undetected, leading to the characteristic signal of dimuonic final states with large missing energy

$$\mu^+\,\mu^- \;\rightarrow\; \mu^+\,\mu^- \;+\not{E}.$$

Standard model processes that produce neutrinos in the final state mimic this signal: most importantly W pair production and t-channel W exchange accompanied by γ, Z^0, or Wradiation leading to two ν_μ's in the final state. We imposed the following requirements on the final state muons to simplify SM background calculations: Their energies ($E_\pm$) must be less than 80 GeV and their combined transverse energy less than 80 GeV; both values are above the maxima in the UED final states over the full range of R^{-1} studied (figure 4). The dimuon invariant mass must be greater than 5 GeV/c^2; this reduces the UED signal by less than 10%, while reducing the photon-mediated pair production background by orders of magnitude. Finally, their angles ($\theta_\pm$) with respect to the incoming beams must be larger than 4°, which is below the minimum shielding angle considered in the studies cited above.

We calculated the SM and UED cross sections with CompHEP [11] using the mUED model of [12]. The SM cross section is 11.4 fb. The UED cross section varies from over two orders of magnitude larger than the background at small R^{-1} to almost an order of magnitude smaller than the background at large R^{-1} (figure 3).

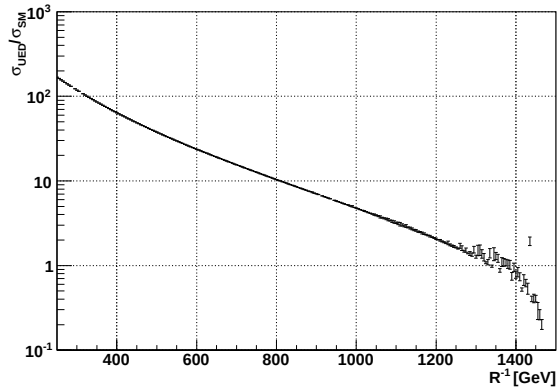

Figure 3: UED cross section compared to SM cross section as a function of R^{-1}.

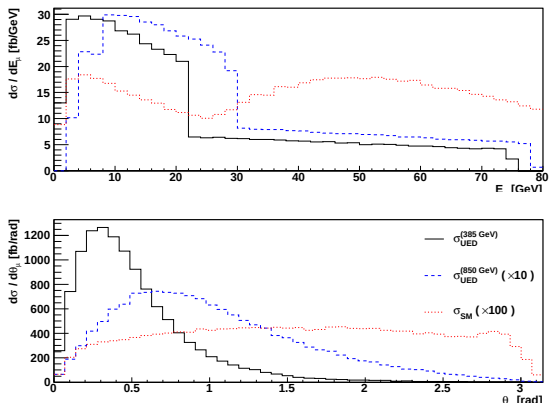

Figure 4: Differential cross section as a function of outgoing muon energy (top) and angle with respect to incoming muon (bottom) for UED and SM.

For $R^{-1} \lesssim 1$ TeV, σ_{UED} is significantly larger than σ_{SM}, and UED discovery is straightforward through measuring the total cross section. At larger R^{-1}, we can exploit differences between the $\mathrm{d}\sigma/\mathrm{d}E_\pm$ and $\mathrm{d}\sigma/\mathrm{d}\theta_\pm$ shapes for UED and the SM (figure 4) to make a discovery. We can achieve this using a binned likelihood analysis in the 4D space $(E_+, \theta_+, E_-, \theta_-)$.

A binned analysis also aids the measurement of R^{-1}. Taking the events in each bin of the $(E_\pm, \theta_\pm)$ space to be Poisson distributed, the log likelihood of a particular value of R^{-1} given a binned set of events $\{n_i\}$ is

$$\ln L = \ln P_0 + \sum_i (n_i \ln \nu_i - \nu_i - \ln n_i!),$$

where P_0 is the prior belief in the value of $R^{-1}$and $\nu_i = \mathcal{L}\sigma_i^{\mathrm{UED+SM}}$ is the expected number of events in bin i for an integrated luminosity $\mathcal{L}$. Taking P_0 to be constant in the vicinity of R^{-1}, the change in $\ln L$ between $(R^{-1} + r^{-1})$

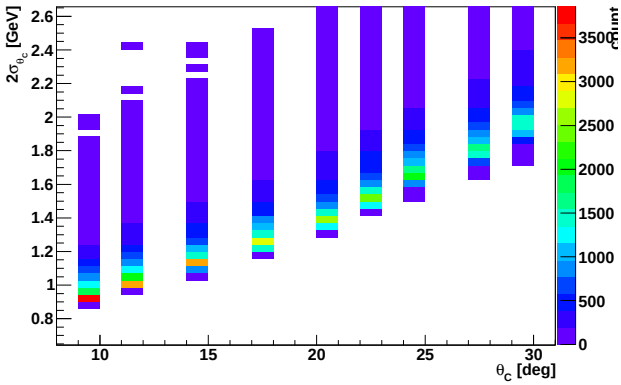

Figure 5: Distribution of 2σ precisions for the measurement of R^{-1} around $R^{-1} = 385$ GeV as a function of shielding angle θ_C for ten-thousand ensemble tests with $\mathcal{L} = 100$ fb^{-1}.

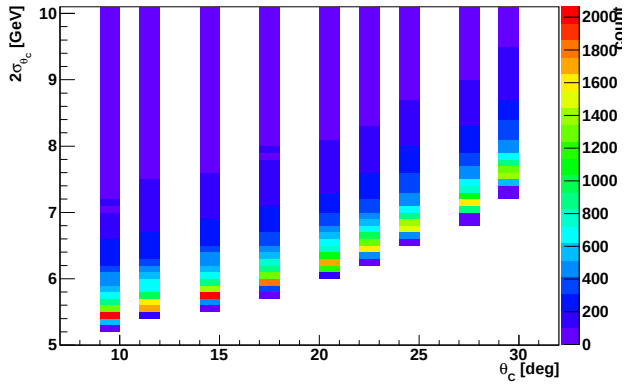

Figure 6: Distribution of 2σ precisions for the measurement of R^{-1} around $R^{-1} = 850$ GeV as a function of shielding angle θ_C for ten-thousand ensemble tests with $\mathcal{L} = 100$ fb^{-1}.

and R^{-1} is

$$\Delta \ln L = \sum_i n_i \ln\left(1 + \frac{\Delta\sigma_i}{\sigma_i}\right) - \mathcal{L}\Delta\sigma_i,$$

where $\Delta\sigma_i$ is the change in cross section in bin i between R^{-1} and $(R^{-1} + r^{-1})$, and σ_i is evaluated at R^{-1}. After Taylor expanding the logarithm to second order in $\Delta\sigma_i/\sigma_i$ and $\Delta\sigma_i$ to second order in r^{-1}, we can calculate r^{-1} as a function of the change of the log likelihood by multiples N^2 of its variance

$$r^{-1}(N) = \frac{\alpha \pm \sqrt{\alpha^2 + N^2\beta}}{\beta},$$

$$\alpha = \sum_i \frac{\sigma_i'}{\sigma_i}(n_i - \nu_i), \qquad \beta = \sum_i n_i \left(\frac{\sigma_i'}{\sigma_i}\right)^2.$$

Evaluating r^{-1} with $N = 2$ gives the 95% confidence (2σ) uncertainty on the measurement of R^{-1}. By performing the sums in α and β with the cut $\theta_C < \theta_\pm < \pi - \theta_C$, we calculate the 2σ R^{-1} precision as a function of the shielding angle θ_C. We calculated the differential cross sections at a central R^{-1} value and several surrounding values within a 10 GeV window. In this window, the σ_i vary linearly, and σ_i' is calculated via a linear fit. Figure 5 shows the results for $R^{-1} = 385$ GeV and $\mathcal{L} = 100$ fb^{-1}: ten thousand data sets ($\{n_i\}$) were generated from the central cross section according to Poisson distributions; plotted is the distribution of 2σ precisions as a function of θ_C for the ensemble tests. The potential precision in measuring R^{-1} is more than twice as fine at 9° than it is at 30°. This precision ratio decreases to 1.5 at $R^{-1} = 850$ GeV (figure 6).

CONCLUSIONS

The angle of the shielding cone around the IP of a muon collider impacts the precision to which the size of a universal extra dimension can be measured, and should have similar effects on other BSM models. Likewise, in a large region of mUED parameter space, discovery potential may be greatly impacted by such shielding. We will continue the above calculations to larger values of R^{-1} in order to make a statement about that impact. The angle of the shielding can be decreased, and thus the performance of the detector in making such BSM measurements improved, by decreasing the beam population. One possibility to achieve this is frictional cooling [13], which can be used to deliver the same luminosity as achieved with ionization colling [14] schemes, common to many muon collider studies, with an order of magnitude fewer muons per bunch [2, 15].

REFERENCES

[1] C. M. Ankenbrandt *et al.*, *PRSTAB*, vol. 2, p. 081001, 1999.
[2] H. Abramowicz *et al.*, *NIMA*, vol. A546, pp. 356–375, 2005.
[3] I. Stumer *et al.*, in *Snowmass 1996*, 1996.
[4] T. Kaluza, *Sitzungsber. Preuss. Akad. Wiss. Berlin (Math. Phys.)*, vol. 1921, pp. 966–972, 1921.
[5] O. Klein, *Z. Phys.*, vol. 37, pp. 895–906, 1926.
[6] G. D. Kribs, TASI 2004 Lecture.
[7] H.-C. Cheng, TASI 2009 Lecture.
[8] T. Appelquist, H. C. Cheng, and B. A. Dobrescu, *Phys. Rev. D*, vol. 64, p. 035002, Jun 2001.
[9] H. Cheng, K. T. Matchev, and M. Schmaltz, *Phys. Rev. D*, vol. 66, p. 036005, Aug 2002.
[10] M. Battaglia *et al.*, *JHEP*, vol. 07, p. 033, 2005.
[11] E. Boos *et al.*, *NIMA*, vol. A534, pp. 250–259, 2004.
[12] A. Datta, K. Kong, and K. T. Matchev, *New Journal of Physics*, vol. 12, no. 7, p. 075017, 2010.
[13] M. Muhlbauer, H. Daniel, and F. J. Hartmann, *Hyperfine Interact.*, vol. 82, pp. 459–467, 1993.
[14] D. Neuffer, *Part. Accel.*, vol. 14, p. 75, 1983.
[15] D. Greenwald, Y. Bao, and A. Caldwell, *AIP Conf. Proc.*, vol. 1222, pp. 293–297, 2010.